Modeling of Resistive Sheets in Finite Element Solutions

J.M. Jin, J.L. Volakis
Radiation Laboratory
Department of Electrical Engineering and Computer Science
University of Michigan
Ann Arbor, MI 48109-2122

C.L. Yu
Pacific Missile Test Center
Pt. Mugu, CA 93042-5000
and
A.C. Woo
NASA-Ames Research Center
Moffett Field, CA 94035-1000

Abstract

A formulation is presented for modeling a resistive card in the context of the finite element method. The appropriate variational function is derived and for validation purposes results are presented for the scattering by a metal-backed cavity loaded with a resistive card.

1 Introduction

A resistive card is an infinitesimally thin sheet of material which allows partial penetration of the electromagnetic field. Thin dielectric layers and very thin conductors whose thickness is less than the skin depth are examples of materials which can be modelled by resistive cards or sheets. Resistive cards are often used for radar cross section and RF power penetration control and as a result they have been studied extensively. Such studies have generally been done in the context of high frequency [1,2] and integral equation solutions [3,4], but to date the treatment of resistive cards within the context of the finite element method (FEM) has not been considered. Over the past few years, FEM has been applied to a variety of electromagnetic applications and it is thus important to incorporate the modeling of resistive cards in the FEM. In this paper we propose an FEM formulation which accounts for the presence of resistive sheets. To validate this formulation, results based on a physical modeling of the resistive sheet are also presented. In this case, the resistive sheet is equivalently replaced by a thin dielectric layer. The modeling of such a layer in the usual manner leads to larger and consequently inefficient linear systems, which is the primary reason for resorting to a mathematical modeling of the resistive sheet. Results based on the mathematical and physical modeling are presented in connection with the scattering by a metal-backed cavity in a ground plane and these are used to validate the proposed mathematical model.

2 Formulation

A resistive sheet is characterized by its resistivity R which is measured in Ohms per square. Mathematically, it satisfies the boundary condition [5

$$\hat{n} \times (\hat{n} \times \mathbf{E}) = -R\hat{n} \times \left(\mathbf{H}^{+} - \mathbf{H}^{-}\right) \tag{1}$$

where $\mathbf{H}^{\pm}$ denotes the magnetic field above and below the sheet, $\mathbf{E}$ is the electric field and its tangential component is continuous across the sheet, and $\hat{n}$ denotes the unit normal to the sheet pointing in the upward direction (+ side). To a first order, this boundary condition can be used to simulate the

presence of a thin dielectric layer by setting [4,5]

$$R = \frac{Z_o}{jk_o(\epsilon_r - 1)t}$$

In this, t is the thickness of the layer, Z_o and k_o denote the free space intrinsic impedance and wave number, respectively, and ϵ_r is the relative dielectric constant of the layer. Alternatively, a resistive sheet may be equivalently replaced by a thin dielectric layer having thickness t and a relative permittivity of

$$\epsilon_r = 1 - \frac{jZ_o}{k_o t R} \tag{2}$$

Generally, the accuracy of this simulation increases as the thickness t is decreased. Typically, t should not exceed one-tenth of the wavelength in the material.

Let us now consider a finite element solution of the fields within a volume V subject to a given excitation. The volume consists of some inhomogeneous dielectric having relative permittivity and permeability ϵ_r and μ_r, respectively, and we shall also assume that resistive cards may be embedded within the dielectric (see Figure 1). In accordance with the finite element method, the volume is subdivided into M smaller volume elements and in this case we require that the resistive cards are tangential to the boundary surface of these elements. A weak solution of the fields within the volume can be obtained by extremizing the functional

$$F = \sum_{e=1}^{M} F^e, \tag{3}$$

$$\begin{aligned} F^e &= \int\int\int_{V_e} \left[\frac{1}{\mu_r} (\nabla \times \mathbf{E}) \cdot (\nabla \times \mathbf{E}) - k_o^2 \epsilon_r \mathbf{E} \cdot \mathbf{E} \right] dv \\ &\quad + jk_o Z_o \oiint_{S_e} \mathbf{E} \cdot (\mathbf{H} \times \hat{n}_e)\, ds \end{aligned} \tag{4}$$

with respect to the electric field $\mathbf{E}$ including that implied in $\mathbf{H}$. In this expression, V_e is the volume of the element which is enclosed by the surface S_e and $\hat{n}_e$ denotes the outward normal to S_e.

Generally, for a dielectric volume not enclosing resistive sheets or other current sheets, the contributions of the surface integrals in (3)-(4) vanish everywhere except when S_e coincides with the outer surface S_o of the volume V. This is a consequence of field continuity across the elements, but if a portion of the element's surface coincides with a resistive sheet, then the surface integral in (4) does not vanish since the magnetic field is discontinuous as described in (1). Let us for example consider the surface S_{re} which borders the eth and $(e+1)$th elements, and is coincident with a resistive sheet of resistivity R. Then the contribution from this surface to the surface integral in (4) is

$$jk_oZ_o \int\int_{S_{re}} \mathbf{E} \cdot \left(\mathbf{H}^- \times \hat{n}_{re}\right) ds$$

from the eth element and

$$-jk_oZ_o \int\int_{S_{re}} \mathbf{E} \cdot \left(\mathbf{H}^+ \times \hat{n}_{re}\right) ds$$

from the $(e+1)$th element with $\hat{n}_{re}$ pointing from the eth to the $(e+1)$th element. Combining these two integrals and employing (1), it follows that the contribution of the surface S_{re} to the surface integral in (4) is

$$\begin{aligned} & - \; jk_oZ_o \int\int_{S_{re}} \left[\mathbf{E} \cdot \left(\mathbf{H}^+ - \mathbf{H}^-\right) \times \hat{n}_{re}\right] ds \\ & = \; jk_oZ_o \int\int_{S_{re}} \frac{1}{R} \left(\hat{n}_{re} \times \mathbf{E}\right) \cdot \left(\hat{n}_{re} \times \mathbf{E}\right) ds \end{aligned} \tag{5}$$

Consequently, the functional F may be rewritten as

$$\begin{aligned} F \; = \; & \sum_{e=1}^{M} \int\int\int_{V_e} \left\{ \frac{1}{\mu_r} \left(\nabla \times \mathbf{E}\right) \cdot \left(\nabla \times \mathbf{E}\right) - k_o^2 \epsilon_r \mathbf{E} \cdot \mathbf{E} \right\} dv \\ & + jk_oZ_o \int\int_{S_r} \frac{1}{R} \left(\hat{n}_r \times \mathbf{E}\right) \cdot \left(\hat{n}_r \times \mathbf{E}\right) ds \\ & + jk_oZ_o \oiint_{S_o} \mathbf{E} \cdot \left(\mathbf{H} \times \hat{n}_o\right) ds \end{aligned} \tag{6}$$

in which S_r denotes the surface occupied by the resistive sheet and S_o is the outer surface enclosing the volume V. As usual, $\hat{n}_r$ is the outward normal to S_r and $\hat{n}_o$ is correspondingly the outward normal to S_o. If S_r borders the

outer surface of the volume V, then S_o should be considered to be just over the exterior side of S_r (i.e., S_o always encloses S_r).

Having derived the explicit form of the functional F, we may now expand the element field using the standard linear shape functions. If the sources are within V then F should be modified to read

$$\begin{aligned} F &= \int\int\int_V \left\{ \frac{1}{\mu_r}(\nabla \times \mathbf{E}) \cdot (\nabla \times \mathbf{E}) - k_o^2 \epsilon_r \mathbf{E} \cdot \mathbf{E} \right\} dv \\ &+ \int\int\int_V \mathbf{E} \cdot \left[jk_o Z_o \mathbf{J}^{int} - \nabla \times \left(\frac{1}{\mu_r} \mathbf{M}^{int} \right) \right] dv \\ &+ jk_o Z_o \int\int_{S_r} \frac{1}{R} (\hat{n}_r \times \mathbf{E}) \cdot (\hat{n}_r \times \mathbf{E}) ds \\ &+ jk_o Z_o \oiint_{S_o} \mathbf{E} \cdot (\mathbf{H} \times \hat{n}_o) ds \end{aligned} \tag{7}$$

where $(\mathbf{J}^{int}, \mathbf{M}^{int})$ denote the impressed sources internal to V. Then, upon setting the first order variation of F to zero, we can obtain a system of equations for the solution of the interior and boundary electric fields. For a unique solution of this system we must, however, specify a relation between the tangential electric and magnetic field which appear in the surface integral over S_o. If we assume that the subject volume is that occupied by the metal-backed cavity recessed in a ground plane, as shown in figure 2, then S_o reduces to the aperture area of that cavity. By invoking image theory, the magnetic field on the aperture can then be expressed as

$$\mathbf{H} = \mathbf{H}^{inc} + \mathbf{H}^{ref} - 2jk_o Y_o \int\int_{S_a} \left[\left(\bar{\mathbf{I}} + \frac{1}{k_o^2} \nabla\nabla \right) G_o(\mathbf{r}, \mathbf{r}') \right] \cdot [\mathbf{E}(\mathbf{r}) \times \hat{z}] \, ds' \tag{8}$$

where S_a denotes the aperture surface, $G_o(\mathbf{r}, \mathbf{r}')$ is the free space scalar Green's function, $\mathbf{r}$ specifies the observation point located on S_a and $\bar{\mathbf{I}} = \hat{x}\hat{x} + \hat{y}\hat{y} + \hat{z}\hat{z}$ is the unit dyad. Also, $\mathbf{H}^{inc}$ denotes the magnetic field generated by sources in the free space and $\mathbf{H}^{ref}$ is the corresponding reflected field when the cavity's aperture is shorted. Substituting (8) into (7) gives a functional only in terms of the electric field. The system obtained from this functional will be partly sparse and partly full. In particular the volume

integrals and that over S_r in (7) lead to a sparse submatrix involving the interior fields of the cavity. However, in view of (8) the last surface integral of (7) over S_o (or S_a) renders a full Toeplitz submatrix since the boundary integral is convolutional. Consequently, by resorting to an iterative solution such as the conjugate or biconjugate gradient method in conjunction with the fast Fourier transform, the need to generate the Toeplitz matrix is eliminated thus maintaining the O(n) storage requirement, characteristic of finite element solutions. The details pertaining to this implementation are discussed in [6] - [8]. In the next section we only present some results aimed at evaluating the accuracy of the proposed resistive sheet model.

3 Numerical Results

Let us consider the metal-backed rectangular cavity illustrated in Figure 2. The cavity is assumed to be empty (no internal sources) and is illuminated by a plane wave in the $\phi = 0$ plane. For implementing the aforementioned solution, the cavity is subdivided into rectangular bricks and the results of the solution are shown in Figure 3. These are radar cross section (RCS) patterns and refer to a 1λ deep cavity whose aperture is also $1\lambda \times 1\lambda$. The RCS pattern in Figure 3(b) applies to the cavity which is loaded with a resistive sheet of $100\Omega/\square$ placed at its aperture, whereas the result in Figure 3(a) is for the untreated empty cavity. The simulation of the resistive sheet was done through direct discretization of the first order variation of the functional F as given in (7) and alternatively by modeling the resistive sheet as a dielectric layer of thickness $\lambda/20$ having the dielectric constant computed from (2). As shown in Figure 3(b) the results based on the two simulations are in reasonable agreement and the differences among them is due to the finite thickness which was necessarily introduced in the physical model of the resistive sheet. As noted in [9] and [10], the dielectric layer introduces vertical components of the electric field which are not present in the resistive sheet. It is certainly of interest to point out that the presence of the resistive sheet at the aperture surface reduced the RCS of the cavity by 10dB at normal incidence and by as much as 20dB at grazing incidence.

The second geometry which was considered is a circular metal-backed cavity again situated in a ground plane. In this case the aperture of the

circular cavity is loaded with a sheet having non-uniform resistivity given by

$$R(\rho) = \begin{cases} Z_o \left[0.1 + 10 \left(\frac{a-\rho}{a} \right)^2 \right] & \rho > 0.5a \\ \infty & \text{elsewhere on } S_a \end{cases} \tag{9}$$

where a denotes the radius of the aperture. Results with and without resistive loading for a cavity having a = 1in. and a depth of 0.25in. are shown in Figure 4. These RCS patterns were computed at 16GHz and the incident field was a plane wave polarized along the θ or ϕ directions. Again, the data in Figure 4 demonstrate the validity of the proposed mathematical model. Also, as in the case of the rectangular cavity the presence of the resistive cards reduces the overall RCS of the cavity and this reduction is primarily due to the reduced field intensity near its perimeter.

4 Conclusions

A formulation was derived for modeling resistive cards within the context of the finite element method. Essentially, the pertinent variational functional was supplemented with an additional boundary integral over the surface of the resistive sheet/card. Results based on the discretization of the functional were also presented and these were aimed at demonstrating the accuracy of the derived mathematical model.

References

[1] T.B.A. Senior, "Scattering by Resistive Strips," *Radio Science*, Vol. **14**, pp. 911-924, 1979.

[2] M.I. Herman and J.L. Volakis, "High Frequency Scattering by a Resistive Strip and Extensions to Conductive and Impedance Strips," *Radio Science*, Vol. **22**, pp. 335-349, May-June 1987.

[3] E.F. Knott and T.B.A. Senior, "Non-Specular Radar Cross Section Study," University of Michigan Radiation Laboratory Technical Report 011764-1-F (also U.S. Air Force Avionics Lab. report AFAL-TR-73-422) January 1974.

[4] R.F. Harrington and J.R. Mautz, "An Impedance Sheet Approximation for Thin Dielectric Shells," *IEEE Trans. Antennas Propagat.*, Vol. **AP-23**, pp. 531-534, 1975.

[5] T.B.A. Senior, "Combined Resistive and Conductive Sheets," *IEEE Trans. Antennas Propagat.*, Vol. **AP-33**, pp. 577-579, 1985.

[6] J.M. Jin and J.L. Volakis, "A Finite Element-Boundary Integral Formulation for Scattering by Three-Dimensional Cavity-Backed Apertures," *IEEE Trans. Antennas Propagat.*, Vol. **AP-39**, pp. 97-104, January 1991.

[7] J.M. Jin and J.L. Volakis, "Electromagnetic Scattering by and Transmission Through a Three-Dimensional Slot in a Thick Conducting Plane," *IEEE Trans. Antennas Propagat.*, Vol. **AP-39**, pp. 543-550, April 1991.

[8] J.M. Jin and J.L. Volakis, "Scattering and Radiation From Microstrip Patch Antennas and Arrays Residing in a Cavity," submitted to *IEEE Trans. Antennas Propagat.*.

[9] T.B.A. Senior and J.L. Volakis, "Sheet Simulation of Dielectric Layers," *Radio Science*, **22**, Dec. 1987, pp. 1261-1272.

[10] J.L. Volakis, "Numerical Implementation of Generalized Impedance Boundary Conditions," 1989 URSI Electromagnetic Theory Symposium, Aug. 1989, Stockholm, Sweden. Symposium Digest pp. 434-437.

FIGURE CAPTIONS

Fig. 1 Cross Section of a dielectric volume enclosing a resistive card (a) card within the dielectric (b) card on the surface of the dielectric

Fig. 2 Geometry of a cavity-backed aperture in a ground plane.

Fig. 3 Monostatic RCS for a rectangular aperture ($1\lambda \times 1\lambda$) backed by a rectangular cavity ($1\lambda \times 1\lambda \times 1\lambda$) in the $\phi=0$ plane. (a) Empty cavity without resistive loading (b) Empty cavity whose aperture is covered with a resistive sheet having a resistivity of $100\Omega/\square$. (Solid and dashed lines correspond to results based on the mathematical simulation; circles and squares refer to results based on the physical modeling of the resistive sheet)

Fig. 4 Monostatic RCS for a circular aperture (1 inch in diameter) backed by a circular cavity (1 inch in diameter and 0.25 inches deep) at 16 GHz. (a) Empty cavity. (b) Empty cavity covered with a resistive sheet whose resistivity is given by equ. (a). (Solid and dashed lines correspond to results based on the mathematical simulation; circles and squares refer to results based on the physical modeling of the resistive sheet)

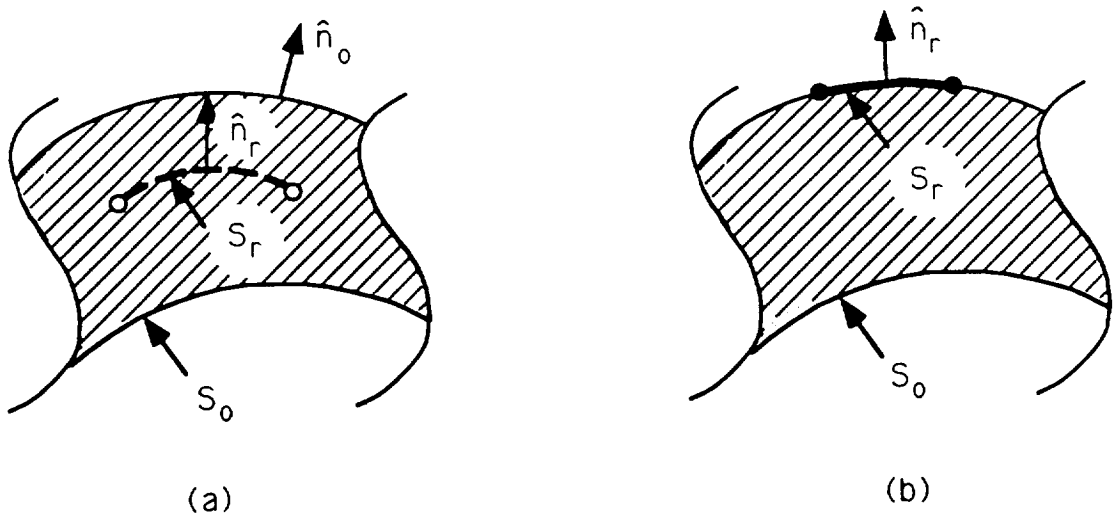

Figure 1. Cross section of a dielectric volume enclosing a resistive card (a) card within the dielectric (b) card on the surface of the dielectric

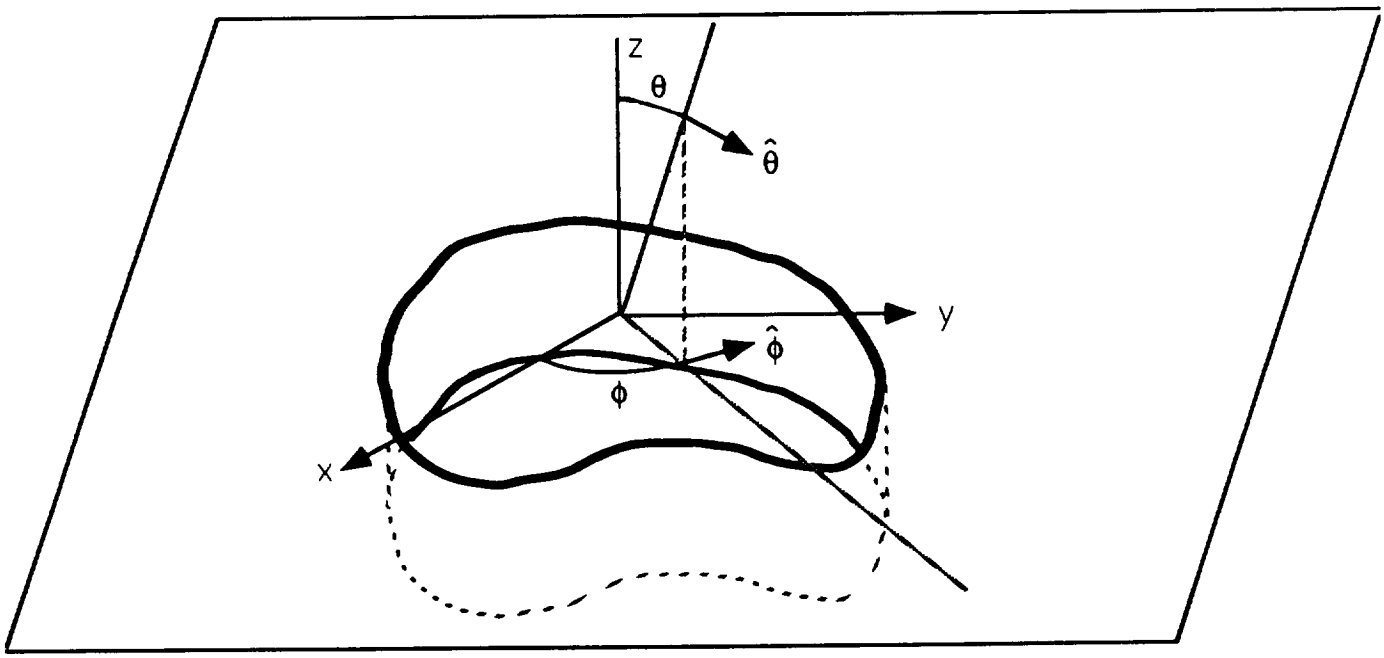

Figure 2

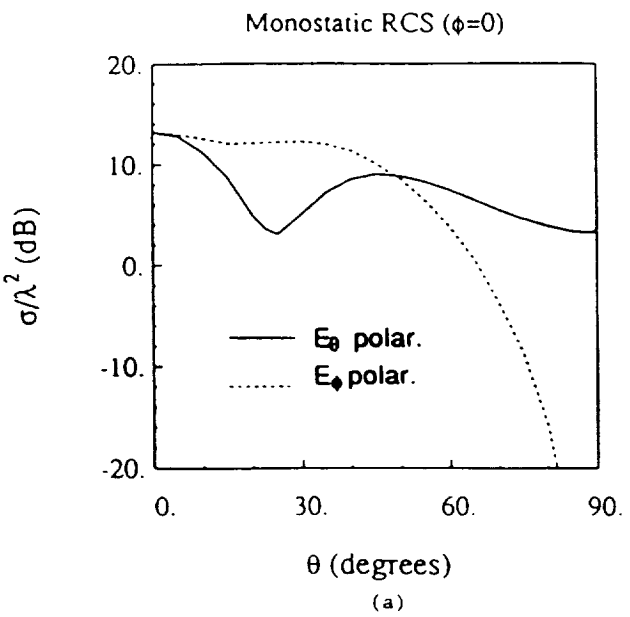

(a)

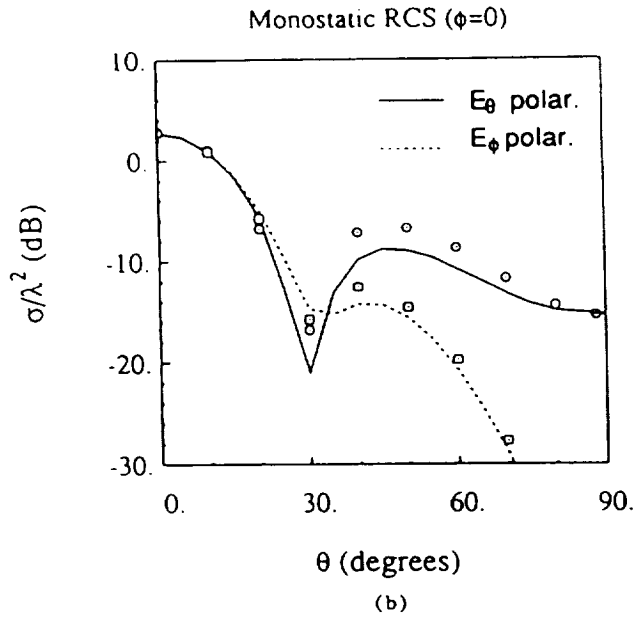

(b)

Figure 3

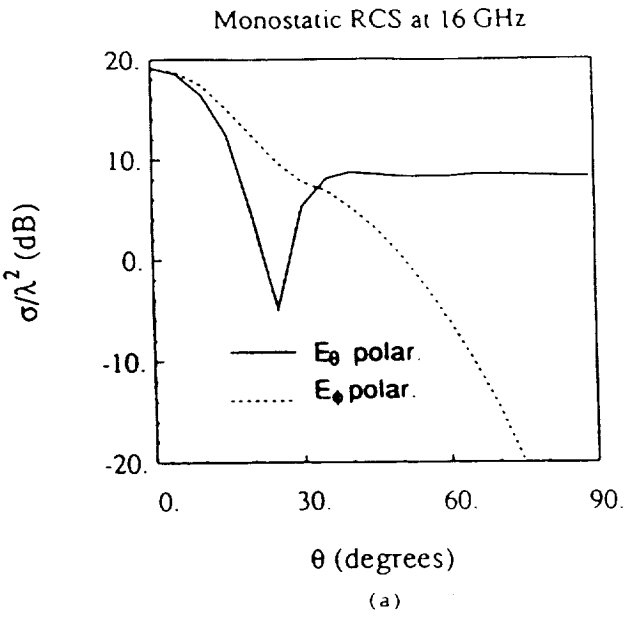

(a)

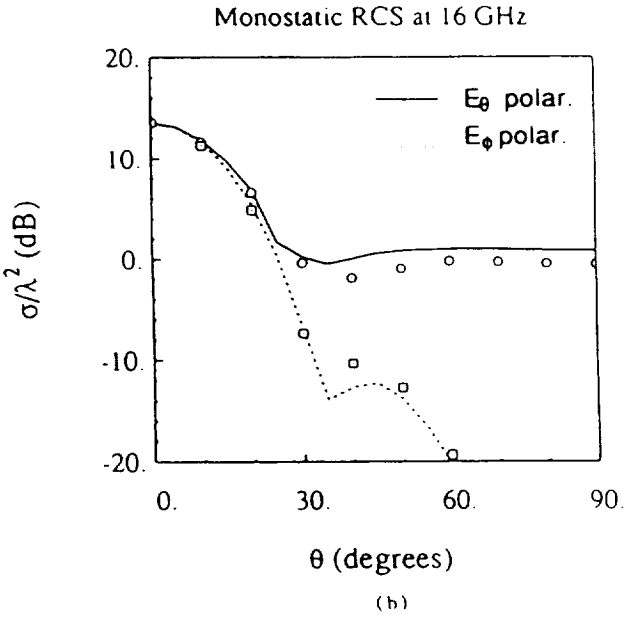

(b)

Figure 4